
LEARNING TO ENGAGE WITH INTERACTIVE SYSTEMS: A FIELD STUDY

A PREPRINT

Lingheng Meng

Electrical and Computer Engineering
University of Waterloo
lingheng.meng@uwaterloo.ca

Daiwei Lin

Electrical and Computer Engineering
University of Waterloo
daiwei.lin@uwaterloo.ca

Adam Francey

Department of Psychology
University of Waterloo
alzfrancey@uwaterloo.ca

Rob Gorbet

Department of Knowledge Integration
University of Waterloo
rbgorbet@uwaterloo.ca

Philip Beesley

Department of Architecture
University of Waterloo
pbeesley@uwaterloo.ca

Dana Kulić

Electrical and Computer Engineering
University of Waterloo
Electrical and Computer Systems Engineering
Monash University
dana.kulic@monash.edu

December 15, 2024

ABSTRACT

Physical agents that can autonomously generate engaging, life-like behaviour will lead to more responsive and interesting robots and other autonomous systems. Although many advances have been made for one-to-one interactions in well controlled settings, future physical agents should be capable of interacting with humans in natural settings, including group interaction. In order to generate engaging behaviours, the autonomous system must first be able to estimate its human partners' engagement level. In this paper, we propose an approach for estimating engagement from behaviour and use the measure within a reinforcement learning framework to learn engaging interactive behaviours. The proposed approach is implemented in an interactive sculptural system in a museum setting. We compare the learning system to a baseline using pre-scripted interactive behaviours. Analysis based on sensory data and survey data shows that adaptable behaviours within a perceivable and understandable range can achieve higher engagement and likeability.

Keywords Living Architecture · Human-Robot Interaction · Reinforcement Learning · Engagement · Voluntary Engagement · Social Robot · Interactive System · Group Interaction · Adaptive System · Natural Setting Interaction · Open-world Interaction · Robotic Arts · Robotic Sculpture

1 Introduction

As robots enter human environments, the importance of engaging with human occupants in a suitable manner becomes increasingly important [1, 2, 3, 4, 5, 6, 7, 8]. To facilitate long-term interaction, interactive systems should be able to continuously adapt in order to generate engaging and appropriate behaviour. Although for simple interactive systems it may be possible to manually design engaging behaviours, this approach is time-consuming and sometimes unfeasible for complex interactive systems. In addition, manually designed behaviours constrain the system to a limited set of reactions, whereas autonomous generation provides the possibility of adaption and continuous behavioural evolution.

Therefore, understanding how to autonomously generate engaging behaviour is necessary for long-term HRI, and learning algorithms can be advantageous.

When introducing learning into an interactive system, human input could be explicit or implicit. An example of explicit input is a human taking a teacher role, giving feedback to guide the robot to achieve some goals. With implicit input, a learning signal is generated based on observations of human behaviours during interaction, without requiring active feedback. For successful long-term interaction in social and public settings, the implicit model is more appropriate than the explicit teacher model, because in the implicit model learning is not dependent on human expertise or willingness to train the system. Finally, for successful interaction in social and public settings, the system should successfully engage with and learn from both individual and group interactions.

We study the challenge of long term autonomy with Living Architecture Systems (LAS). LAS are interactive systems at architectural scale that emulate living environments aiming to engage occupants in long-term interaction (see Fig. 1 for sample installations by the Living Architecture Systems Group (LASG) and Philip Beesley Architect Inc. (PBAI)¹). An immersive LAS can have dozens of sensors and hundreds of actuators with various modalities to enable interaction with visitors, which poses a challenge when designing effective interaction control strategies. Historically LASG/PBAI environments have used pre-scripted, human-designed behaviours. In this work, we are interested in the potential for adaptive machine learning behavioural algorithms to generate interactive behaviours. LAS aims for long-term continuous interaction, and this necessitates the capability of LAS to evolve with and to learn in a non-stationary environment, rather than using a single pre-scripted solution or assuming the existence of a single optimal solution.



(a) *Radiant Soil*, installed in Daejeon Museum of Art in Daejeon, South Korea, 2018.

(b) *Epiphyte Spring*, installed in Design Institute of Landscape and Architecture in Hangzhou, China, 2015.

(c) *Hylozoic Series: Sibyl*, installed in the Industrial Precinct in Sydney, Australia, 2012.

Figure 1: Living Architecture Systems. (Photos courtesy of Philip Beesley Architect Inc.)

Although LAS aims for long-term engagement with occupants, the architectural scale and non-anthropomorphic, immersive nature of LAS makes it distinctive compared to robots more typically studied in HRI [9, 10, 11, 12, 13, 14]. Since LAS is intended to create lifelike behaviours at architectural scale, it facilitates accommodating multiple occupants and group interaction, rather than one-to-one interaction most commonly studied in HRI. In addition, unlike HRI studies with humanoid robots that can be directly inspired by human-human interactions, LAS is a non-anthropomorphic robot, making it less intuitive to design interactive behaviour. While it is possible to manually design lifelike interactive behaviours to some extent, it is very time-consuming, and the resulting behaviours are non-adaptive. Therefore, implementing interactive systems that can adapt and learn in dynamic crowd settings and can autonomously generate engaging behaviour is critically important, not only because it is useful in many applications, including public spaces, schools, workplaces, and family residences etc, but also because HRI in such interactive systems could extend our understanding of socially acceptable and engaging interactive behaviour.

Manually designed behaviour patterns can generate engaging lifelike behaviours based on the designer’s understanding [15, 16], but this can be time-consuming and result in behaviours that become predictable during long term interaction. To overcome this limitation, machine learning may be used to automatically generate behaviour and study whether such behaviour is attractive or engaging for participants. For example, in [17, 18], a Curiosity-Based Learning Algorithm (CBLA) was implemented in the LAS to automatically generate behaviour based on a computational notion of curiosity [19] of the LAS. However, the action produced by the CBLA is purely intrinsically motivated by the curiosity mechanism and does not consider any extrinsic motivation, e.g., maximizing measures of human response, which could play a more important role when an interactive system aims to engage participants. Another issue with [17, 18] and many works on social robots [11, 20] is that the proposed approach is only designed and tested for one-to-one interaction in a controlled

¹More LAS environments by LASG/PBAI can be found at <http://www.philipbeesleyarchitect.com/sculptures/>

setting, rather than group interactions in natural settings, i.e., multiple people interacting with an interactive system simultaneously without instruction or guidance by the researchers.

Learning interactive behaviour for an extrinsically motivated LAS in natural settings with group interactions is a difficult challenge that is not typically considered in Reinforcement Learning (RL) tasks in controlled settings with only one-to-one interaction. Firstly, LAS is an interactive system at architectural scale, with very large state and action spaces, typically having dozens of sensors and hundreds of actuators. The learning challenge is exacerbated by a complicated and non-stationary environment, where the LAS might be manipulated by occupants and occupants might have different cultural backgrounds, interests and personalities. In addition, interactions happening in the real world happen less frequently than interactions in the simulators or video games typically studied in RL. This results in fewer interactions, which poses a huge challenge for data-driven learning algorithms. Last but not least, there is no standard measurement for estimating engagement, i.e., the extrinsic motivation of LAS. If a measurement of engagement is sparse and time-delayed, learning interactive behaviour becomes more difficult.

In this paper, we investigate extrinsically motivated learning in natural settings with group interaction. Specifically, we use sensors embedded in the interactive system to estimate the overall occupancy and engagement of the visitors in the LAS, and use this estimate as the extrinsic reward for learning. We investigate how different formulations of the action-space impact learning, and in particular, whether we can exploit the designer’s pre-scripted behaviours to bootstrap learning. We use the Deep Deterministic Policy Gradient (DDPG) algorithm to train an Actor-Critic agent which acts either in the designer-parameterized action space, which we call the Parameterized Learning Agent (PLA), or in the raw actuator space, either as a single agent (called Single Agent Raw Act, SARA), or as a group of agents (called Agent Community Raw Act, ACRA). We compare the learning agents’ performance to the human-designed, pre-scripted behaviours (PB), using our sensor-based measure of engagement. These four behaviours are evaluated over three weeks at a public exhibition at the Royal Ontario Museum (ROM), and all data is collected from museum visitors. We evaluate how engaging the behaviours are based on a quantitative analysis of estimated engagement and the number of active interactions, and on qualitative analysis of human survey results.

2 RELATED WORK

A number of previous works have considered reinforcement learning in the context of human-robot interaction. During interaction, RL can be used to autonomously adapt robot behaviour to different personalities or environments. [21] applied RL in a complex human online social environment, where a human interacts with a learning agent by providing a reward signal, and highlighted that many of the standard assumptions, such as stationary rewards, Markovian behaviour, appropriateness of average reward, for RL are clearly violated. [22, 23] presented Interactive Reinforcement Learning (IRL) for training human-centric assistive robots through natural interaction, where a human coach’s feedback is used to shape the predefined reward. In addition, [22, 23] introduced anticipatory cues to allow the human coach to predict the robot’s action and provide timely feedback. In [24], IRL was first studied in real-world robotic systems, and showed that the positive effects of human guidance increase with state space size. Other works converting human feedback to reward include [25, 26]. [27] proposed an algorithm (Advise) to formalize the meaning of human feedback as policy feedback, which is more effective and robust than using human feedback as extra reward. [28] investigated the effectiveness of using RL to learn socially acceptable approaching behaviour for a mobile robot. [29] studied the effect of different teaching methods with the same underlying RL algorithm on human teachers’ experience in terms of frustration. This work emphasizes that high transparency will decrease frustration and increase perceived intelligence. In [30], emotion recognition based on videos captured during participants’ interaction with a robot is exploited as a reward within an RL framework to adapt the robot’s behaviour towards participants’ personal preferences. Different from most of these works where the human plays the direct role of teacher, i.e., directly providing either a reward or a policy advice in an interactive way, in this paper we aim to learn how to engage visitors without requiring them to consciously teach or train the interactive system, similar to [30]. Therefore, in this paper the learning agent does not explicitly receive rewards from visitors, but uses a measure of engagement as reward, which is calculated based on observed visitor behaviours, without any constraints on the frequency and consistency of interaction on the visitor.

Interactions in natural settings, e.g., public spaces, are too complex to be simulated in controlled laboratory settings, so to understand natural HRI it is necessary to conduct field studies. Many human-robot interaction systems have been tested in public spaces such as hospitals [31], train stations [32], service points [33], airports [34], shopping malls [35], hotels [36] and museums [37], among others. Although robots investigated in these papers are sometimes surrounded by a group of people in a public place, these robots typically interact with only one person at a specific time, i.e., one-to-one interaction. Unlike these works, the larger scale of LAS enables LAS to simultaneously accommodate interactions with multiple people. In addition, the behaviours of robots studied in most of these works are pre-designed by researchers without continuous learning and adaptability.

As the intention of HRI is to engage human participants in interactions, detecting and measuring initial and ongoing engagement in HRI is critical for initiating and maintaining interaction. Many approaches for measuring engagement rely on rich sensors, such as cameras, lasers, sonar and audio sensors, and on sophisticated facial expression, gesture, gaze and speech recognition technologies [38, 7]. Doherty et al. [39] reviewed the definitions, theory and measurement of engagement mainly from the perspective of human computer interaction (HCI), Glas et al. [40] from the perspective of human-agent interaction, while O’Brien and Toms [41] reviewed the factors affecting user-system interaction from a more general perspective. [42] studied a spatial model of engagement for a social robot and tested a robotic receptionist to engage visitors, and suggested that direction and speed of motion are more appropriate measures of engagement than location or distance alone. However, this work used distance to determine the engagement level and what pre-scripted behaviour to take, rather than using the distance as a learning signal. [43, 44] studied the engagement model for a multiparty open-world dialog system, but the system can only actively engage in at most one interaction even though it could simultaneously keep track of additional, suspended interactions. Engagement in [43, 44] is viewed as several states. Behaviours corresponding to each engagement state are pre-defined. Even though the authors claim the system is a multiparty interaction, the number of participants is limited because of the field of view of the camera and the interaction screen. Most works studying engagement in HRI focus on humanoid social robots, one-to-one interactions, and discrete measures of engagement. In this paper we study a non-anthropomorphic robotic environment, group interaction, and measure engagement as a continuous value. Most importantly, we use a measure of engagement as the extrinsic reward to drive learning, rather than using the measure of engagement as a contingent event to trigger a predefined behaviour.

Interactive artworks are outcomes of combining arts and engineering, and have brought a new research direction for understanding HRI, especially with non-anthropomorphic robots, not only from the robotics perspective but also from an artistic perspective. LAS in this paper and previous installations [16] are examples of such immersive interactive systems that promote roboticists’ and architects’ understanding of lifelike interactive behaviour. Other examples include [45], who investigated visitors’ interaction and observation behaviours with mobile pianos in a museum. [46, 47] studied flying cubes in multiple publicly accessible spaces where flying cubes play the role of living creatures. In [48], roboticists collaborated with a professional dancer to design interactive dancing robots. [49] created spatial interactions with immersive virtual reality technology. [50] studied dancing quadcopters, without an interactive component. Close collaboration between artists and roboticists has been fostering the creation of richer modes of interaction and extending the scope of studies in HRI. Most works mentioned here rely heavily on the design of choreographers, while in this paper we add adaptability on top of choreography by learning engaging behaviour based on the action space defined by choreographers.

Interactive systems, whether humanoid robots or non-anthropomorphic robots like LAS, are human oriented and aim for continuous engagement. These characteristics intrinsically require agents to be able to autonomously generate behaviours and continuously adapt to their human partner(s). In this paper, we exploit the standard reinforcement learning (RL) framework and a novel reward function estimating engagement to realize autonomous agents, and study if this reward could generate behaviour that is more engaging than pre-scripted behaviour. In addition to learning on top of parameterized action space, we also investigate learning directly on raw actuator spaces. All experiments are conducted in a public museum exhibit with museum visitors.

3 The Interactive Architecture Testbed

In this section, we describe the physical system used as the test-bed in this paper, and the design of *Pre-scripted Behaviours (PBs)* that drive the interactive behaviour of the system. The PBs, which are designed by expert architects and interactive system designers, are the baseline we use to compare to the learning systems described in Section 4 below.

Our testbed is the installation called *Transforming Space*, as shown in the top-left sub-figure in Fig. 2, which was exhibited at the Royal Ontario Museum (ROM) in Toronto, Canada from June 2 to October 8, 2018 (<https://www.rom.on.ca/en/philip>). The installation consists of the Canopy and Sphere, which are both publicly accessible to visitors of the museum.

Since this work mainly used the Canopy part of the installation, we will describe the design of the Canopy in detail, and subsequently refer to the Canopy part of the installation as the Living Architecture System (LAS).

3.1 Physical Living Architecture System

The LAS hangs overhead within the Canopy space, with an approximate height of 1.8 meters. Fig. 2 shows the front view of the LAS. The system is composed of eight speakers and 24 nodes.

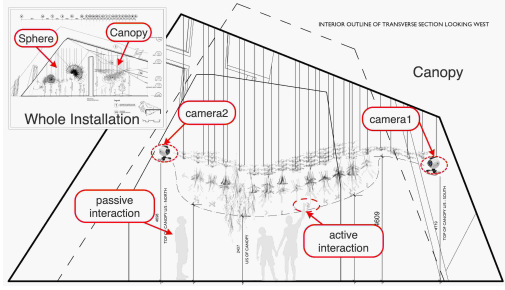


Figure 2: Installation Diagram and Interaction Types

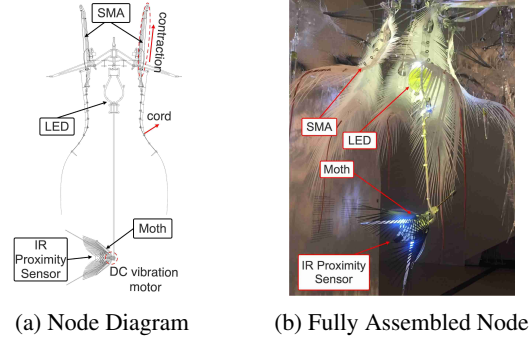


Figure 3: Diagram of Node in the LAS

Each node in the LAS consists of six Fronds, one Moth, and one high-power LED as its actuated systems and one infrared (IR) sensor, as shown in Fig. 3. Each Frond includes a shape memory alloy (SMA) wire which contracts when voltage is applied, pulling a cord attached to a flexible co-polyester sheet, as illustrated in Fig. 3a. The contraction generates a smooth and gentle movement, and when the applied voltage is removed the SMA slowly relaxes to its original shape.² The Moth consists of wing-like flexible flaps attached to a small DC vibration Motor that vibrates when activated, making the moth appear to be flapping its wings. The Moth also houses two small LED lights which illuminate during vibration. The single high-power LED located beneath the central flask can be faded to illuminate the coloured liquid in the flask. The IR sensor senses the proximity of visitors, and generates a continuous reading proportional to the distance between any part of the body of a visitor and the sensor location in the canopy.

There are eight speakers distributed throughout the LAS. These speakers play two types of sound samples. The first sound is a background sound played on a continuous loop. The second sound is triggered by the IR sensors. These speakers are independently controlled by specialized software, so here we treat them as background behaviours.

The arrangement of the speakers and nodes is illustrated in Fig. 4, where the 24 nodes are highlighted by red circles. A photo of the physical LAS is shown in the bottom-left of Fig. 4. The 24 nodes are at varying height levels. Specifically, nodes at the left and right edges are slightly higher than those in the middle of the LAS. This spatial arrangement distinguishes three types of visitor engagement with the system. When visitors observe the LAS but are not underneath the LAS, no IR sensor is activated, i.e., visitors are observing the LAS but cannot be observed by the LAS sensors. As shown in Fig. 2, when visitors walk or stand underneath the LAS, which we name *Passive Interaction*, the IR sensors above them are activated, but the distance between the visitor and the system is still large, corresponding to a small reading of the IR sensor. Visitors engaging in *Active Interaction* might also reach their hand upwards to interact with the LAS, resulting in a higher activation value of the closest IR sensor.

Two web cameras (labeled Camera1 and Camera2 in Fig. 2 and Fig. 4) are used to record video during our experiment and to calibrate sensory data. These two web cameras are mounted on the wall in the front-right and back-left corners of the LAS space.

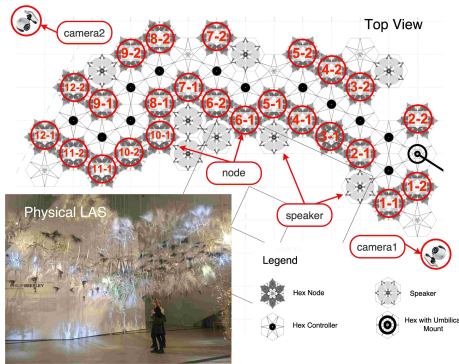


Figure 4: LAS: Canopy

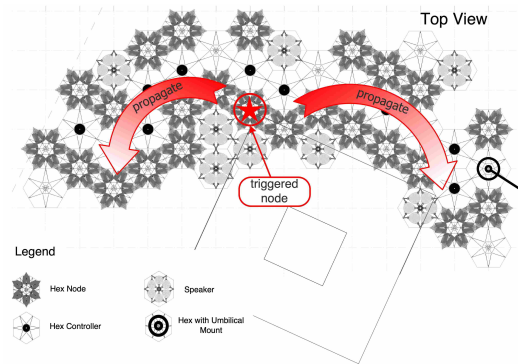


Figure 5: Pre-scripted Behaviour

²A video illustrating the SMA assembly contracting and relaxing can be found in <https://youtu.be/YcreirXrRF4>.

3.2 Pre-scripted Behaviour

Pre-scripted behaviour (PB) is the interactive behaviour manually designed by the architects, and it is also the baseline used for comparison with adaptive behaviours we will describe in Section 4. Within the PB mode, the system can be in two types of states: active and background, which are mainly controlled by 17 parameters (shown in Table 1) specified by the architects. The values in the Default and Range columns are used in the PB and PLA modes, respectively.

In PB, if any of the IR sensors is triggered, the system enters the active state. In this state, the node corresponding to the triggered sensor will first activate its *local reflex behaviour*. In the local reflex behaviour, the Moth, the LED and six SMAs attached to the same node as the triggered IR sensor will be activated. When a Moth is activated, it will gradually increase the vibration (T_{ru}^m) to its maximum (I_{max}) and then keep vibrating for a period of time (T_{ho}^m). After that, it gradually stops (T_{rd}^m). After a waiting period (T_{gap}^m) following the sensor trigger, the LED on the same node is activated. It ramps up (T_{ru}^l) to its maximum brightness (I_{max}), holds (T_{ho}^l) and then gradually dims (T_{rd}^l). At the same time, the SMAs are activated one after another separated by (T_{gap}^{sma}). A voltage is applied to contract the SMA, after which a cooling-down time is started during which this SMA will not be activated again. The activation profile of the SMA wires is fixed in order to protect them from overheating, so these are not included in the parameterization shown in Table 1. Meanwhile, this detected event will be propagated from the triggered node to neighbouring nodes (T_{gap}^n) until the edge nodes of the LAS are reached (shown in Fig. 5), causing a cascade of local reflex behaviours at each node.

If no IR sensor triggering happens for a random time within ($T_{bg}^{min}, T_{bg}^{max}$), the system goes into the background state. In this state, the LED and SMA will activate their local reflex behaviours every random amount of time (T_w, T_{sma}) with probability (P). The choice of activating LEDs and SMAs are independent.

In either state, a sweep of LEDs along the longer axis in either direction of the installation happens every random amount of time ($T_{sw}^{min}, T_{sw}^{max}$). During the sweep, each LED activates local reflex behaviour and propagates in the direction of the sweep.

Table 1: Pre-scripted Behaviour Parameters

Parameters	Meaning	Default	Range
T_{ru}^m, T_{ru}^l	ramp up time: the time it takes for the Moths or LEDs to fade up to their maximum value	1.5	[0, 5]
T_{ho}^m, T_{ho}^l	hold time: the time that Moths and LEDs are held at their maximum value	1	[0, 5]
T_{rd}^m, T_{rd}^l	ramp down time: the time it takes for Moths and LEDs to fade down to 0	2.5	[0, 5]
I_{max}	maximum brightness of LEDs	200	[0, 255]
T_{gap}^m	the time gap between the Moth starting to ramp up and the LED starting to ramp up	1.5	[0, 5]
T_{gap}^{sma}	the time gap between activation of each SMA arm on the nodes	0.3	[0, 5]
T_{gap}^n	the time gap between activation of each node	1.8	[0, 5]
T_{bg}^{min}	minimum time to wait before activating background behaviour	45	[15, 60]
T_{bg}^{max}	maximum time to wait before activating background behaviour	90	[60, 100]
T_w	time to wait before trying to pick a moth or LED	5	[0, 10]
P	probability of successfully choosing an actuator	40	[0, 100]
T_{sma}	time between choosing SMAs to actuate	0.7	[1, 5]
T_{sw}^{min}	minimum time to wait before performing sweep	120	[5, 200]
T_{sw}^{max}	maximum time to wait before performing sweep	240	[200, 400]

The unit of all time parameters is seconds, except I_{max} does not have unit and P is percentage.

4 PROPOSED APPROACHES

In this section, we will describe how the three adaptive behaviour modes, i.e., *Parameterized Learning Agent (PLA)*, *Single Agent Raw Act (SARA)* and *Agent Community Raw Act (ACRA)*, are designed to automatically generate interactive actions. All the adaptive behaviours use a standard reinforcement learning framework and share the same extrinsic

reward formulation estimating the occupancy and engagement level of visitors based on IR sensors. The three learning methods are differentiated by the choice of state and action space.

4.1 Estimating and Using Engagement as a Reward for Learning

A key feature of our approach is the formulation of the reward function: we wish to learn and reward behaviours which foster visitor engagement. Specifically, the extrinsic reward is computed by summing over the IR observations, which can be regarded as a rough estimate of occupancy and engagement, because: 1) more activated IRs means more people are standing under the LAS, thus indicating higher occupancy; 2) closer distance between visitors and IR sensors implies more active interaction, e.g., looking very closely or raising hands, which are higher engagement behaviours. Therefore, higher occupancy and more active interaction will cause higher extrinsic reward. Formally, given a new observation at time $t + 1$, $\mathbf{obs}^{(t+1)} = (\mathbf{obs}_1^{(t+1)}, \mathbf{obs}_2^{(t+1)}, \dots, \mathbf{obs}_n^{(t+1)})^3$, where the value of n depends on the specific behaviour mode, the reward $r^{(t)}$ for taking action $\mathbf{a}^{(t)}$ while observing $\mathbf{obs}^{(t)}$ can be expressed as Eq. 1:

$$r^{(t)} = \sum_{i=1}^n \mathbf{obs}_i^{(t+1)}. \quad (1)$$

The definition of the observation and action spaces for each adaptive behaviour is detailed in the following subsections.

4.2 Parameterized Learning Agent: Learning on Top of Pre-scripted Behaviour

The first adaptive behaviour, PLA, is designed to learn on top of PB, i.e., parameterized action space. The motivation for this approach is to bootstrap learning by exploiting the designer’s knowledge of engaging behaviour, where we hypothesize the designer already has a good idea about what types of actions might be engaging to visitors and this can form a helpful starting point for the learner.

For PLA, we select 11 parameters from Table 1 as the action space, i.e., the dimension of the action vector is 11. This is because some parameters don’t take effect until a subsequent trigger or until the current propagation finishes. This could lead to obtaining an observation which is based on both previous and updated parameters. To avoid this issue, we exclude T_{bg}^{min} , T_{bg}^{max} , T_w , P , T_{sw}^{min} and T_{sw}^{max} from the action space. In this way, we make sure every observation is only related to the latest action. To attenuate IR sensor noise, the observation for PLA is an average over 20 IR readings as defined in Eq. 2:

$$\mathbf{obs}^{(t)} = \frac{1}{20} \sum_{i=0}^{19} \mathbf{ir}^{(t-i*\Delta t)} \quad (2)$$

where $\mathbf{ir}^{(t-i*\Delta t)}$ is the value array of 24 IR sensor readings at time $(t - i * \Delta t)$, \sum is element-wise summation, and $\Delta t \approx 0.1s$ is the time to retrieve one set of 24 IR values from the physical LAS. Thus the dimension of the observation vector is 24 and each observation vector represents the average IR readings over 2 seconds. Based on the observation, the extrinsic reward for PLA is calculated according to Eq. 1 where n is 24. For additional implementation details, please refer to Appendix A.1.1.

4.3 Single Agent Raw Act: Learning in Raw Action Space

SARA investigates the performance of the learner when directly controlling raw actuators without exploiting human expertise. In this fully automated approach, we want to observe how learning evolves when the learner has no access to human expertise, given a large action space and sparse observation space.

SARA directly controls the 192 raw actuators of the LAS using a single agent. Unlike PLA, SARA does not have any trigger-based propagation behaviour, so SARA could execute actions at a higher frequency. Thus, the observation vector $\mathbf{obs}^{(t)}$ of SARA is a concatenation of 5 IR readings as shown in Eq. 3,

$$\mathbf{obs}^{(t)} = [\mathbf{ir}^{(t-0*\Delta t)^T}; \mathbf{ir}^{(t-1*\Delta t)^T}; \dots; \mathbf{ir}^{(t-4*\Delta t)^T}]^T \quad (3)$$

where $\mathbf{ir}^{(t-i*\Delta t)}$ is a vector of 24 IR sensor readings at time $(t - i * \Delta t)$, and $\Delta t \approx 0.1s$ is the time to retrieve one set of 24 IR values from the physical LAS. Thus the dimension of the observation vector $\mathbf{obs}^{(t)}$ is $120 = 24 \times 5$. IR readings are sampled at a frequency of around 10Hz, so actions can be taken at approximately 2Hz. The reward is calculated according to Eq. 1, with $n = 120$. For more implementation details, please refer to Appendix A.1.2.

³In this paper, we will use normal lowercase for scalar and bold lowercase for vector.

4.4 Agent Community Raw Act: Distributed Multi-agent Learning System

In addition to no accessible human expertise, ACRA controls the raw actuators in a decentralized way, where a distributed multi-agent learning system replaces the single large learner in SARA. This approach, compared with SARA, enables: 1) reducing the dimension of the action and observation spaces, and 2) investigating whether cooperating and competing behaviour will emerge among agents as in other multi-agent systems [51].

In ACRA, the physical system is manually decomposed into three sub-systems (as shown in Fig. 6), and each sub-system is independently controlled by an agent in the agent community. The decomposition strategy shown in Fig. 6 is a simple spatial grouping. Concretely, each agent in the agent community monitors eight IR sensors and controls $8 \times (6 \text{ SMAs} + 1 \text{ LED} + 1 \text{ Moth}) = 64$ actuators. The observation of each agent in ACRA is a concatenation of 5 samples of the eight IR sensors under its control as shown in Eq. 4

$$\mathbf{obs}_{agent}^{(t)} = \left[\mathbf{ir}_{agent}^{(t-0*\Delta t)^T}; \mathbf{ir}_{agent}^{(t-1*\Delta t)^T}; \dots; \mathbf{ir}_{agent}^{(t-4*\Delta t)^T} \right]^T \quad (4)$$

where $\mathbf{ir}_{agent}^{(t-i*\Delta t)}$ is the value array of IR sensor readings under the control of *agent* at time $(t - i * \Delta t)$, and $\Delta t \approx 0.1s$ is the time to retrieve one set of 24 IR values from the physical LAS. Thus the dimension of each agent's observation space is $40 = 8 \times 5$. The reward for each agent in ACRA is calculated according to Eq. 1 with $n = 40$. Each agent in ACRA is implemented with the same structure as that used in SARA. For more implementation details, please refer to Appendix A.1.3.

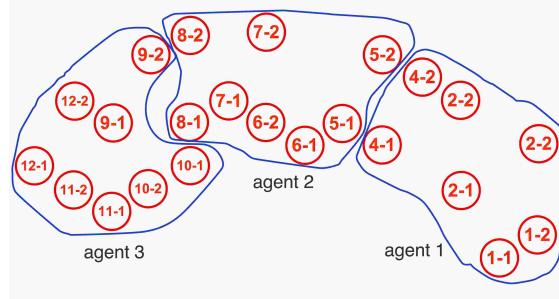


Figure 6: Agent Community Partition

The differences among these three adaptive behaviours are the design of the observation and action space as summarized in Table 2.

Table 2: Observation and Action Space of Four Behaviour Modes

Behaviour Mode	Observation Space Dimensions	Action Space Dimensions
PB	n/a	n/a
PLA	24	11
SARA	$24 \times 5 = 120$	$24 \times (6 + 1 + 1) = 192$
agent in ACRA	$8 \times 5 = 40$	$8 \times (6 + 1 + 1) = 64$

4.5 Overall Learning Framework

Given the observation and extrinsic reward, the learning can be implemented by any Reinforcement Learning algorithm⁴. In this paper, learning is implemented using the Deep Deterministic Policy Gradient (DDPG) algorithm[52]. DDPG is a variant of Deterministic Policy Gradient[53], where both the Actor and Critic are approximated with deep neural networks. We chose DDPG for each adaptive behaviour because: 1) the action space is continuous, and compared with benchmarks reported in the literature [54] [55] the dimension of action is relatively large, which means even if we discretize the continuous action, the dimension of the discretized action space will be very large; 2) compared with other RL algorithms for continuous action space, DDPG is easier to implement. Detailed neural network structures used in this paper for each adaptive behaviour can be found in Appendix A.1.

⁴However, not that the interaction frequency is limited by the physical constraints of the LAS.

4.6 Hypotheses

Our hypotheses are the following:

H1. *Learned interactive behaviours result in higher engagement and perceived likeability than pre-scripted behaviours.*

H2. *Learning in the designer-provided parameterized action space results in higher engagement than learning using the raw actuator action space.*

To validate these hypotheses, we compare the observed interactions during pre-scripted and learning agents based on three criteria: 1) the estimated engagement level (Section 5.4.4), 2) the number of active interactions (Section 5.4.5), and 3) the perceptions of the systems based on human survey data and researchers' observation in Section 6.

5 EXPERIMENTS

5.1 Experimental Procedure

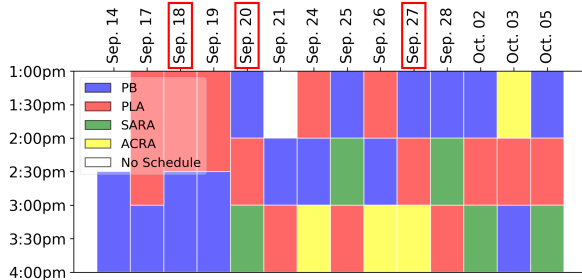
Our experiment was conducted for two weeks from Sept. 14 to Oct. 03, 2018, at the ROM. We were permitted by the ROM to collect data from 1 p.m. to 4 p.m. every day on weekdays. In addition, we conducted in-person surveys on Sept. 18, 20, and 27. During the entire experiment period, visitors were free to visit and interact with the installation without any interference from researchers.

For each day of the experiment, the following procedure was followed:

1. Randomly schedule the different agent conditions into 1 or 1.5 hour time slots as shown in Fig. 7. PB and PLA were scheduled on each day, while only one of SARA and ACRA were scheduled per day.
2. Automatically run scheduled behaviour at each time slot, and save interaction data and learned models and videos at the end of each behaviour.

During days where no visitor surveys were collected, researchers were not present in the environment. During the three survey days, researchers were present, but did not provide any additional instructions to visitors. Researchers observed which visitors interacted with the LAS, passively or actively, within a specific behaviour period. When visitors were finished with their visit, researchers unobtrusively approached randomly selected visitors who had interacted with the system, and asked them if they were willing to participate in a survey. If a visitor agreed to do the survey, they were guided to a table located around a corner and were provided with a tablet with a questionnaire (see Section 5.2). The researchers also recorded which mode the visitor had interacted with. We only recruited visitors who had interacted with only one behaviour mode.

The overall experiment schedule is shown in Fig. 7, where red, blue, green, yellow and white areas correspond to PB, PLA, SARA, ACRA and no schedule respectively. A summary of the experiment schedule and collected data is shown in Table 3.



Video was not available on Sep. 14.

Figure 7: Experiment Schedule

Table 3: Summary of Experiment Schedule and Data

Behaviour	Days	Hours	Survey Participants
PB	13	16.5	14
PLA	13	15.5	15
SARA	4	4	4
ACRA	4	4	3

Video was not available on Sep. 14.

5.2 Data Collection

The data collected comes in four types: sensor readings, learning agent logs, human survey data and video data from the two web-cams.

Every raw sensor reading is logged. In addition to the raw sensor data, each agent also logs its own learning algorithm data collected during the course of learning.

For human survey data, 14, 15, 4, and 3 participants completed surveys in the PB, PLA, SARA and ACRA modes respectively, as summarized in Table 3. The questionnaire used in our experiment is a standardized measurement tool for HRI: the Godspeed questionnaire [56]. In addition to the 24 Godspeed questions, we asked participants about their interests and background, and their general feedback and comments. The Questionnaire consists of four types of questions:

1. Participants' interests and background (multiple-select multiple choice);
2. Participants prior knowledge about interactive architecture and machine learning, including "How familiar are you with interactive architecture?" and "How familiar are you with machine learning algorithms?";
3. 24 Godspeed questions namely Godspeed I: Anthropomorphism, Godspeed II: Animacy, Godspeed III: Likeability, Godspeed IV: Perceived Intelligence and Godspeed V: Perceived Safety [56];
4. Participants' general feedback, i.e., "Any additional comments regarding your experience?" and "Any overall feedback?".

Video data is collected to calibrate sensory readings and validate occupancy estimates, which will be discussed in detail in Section 5.4. Video data is available for all the experiments except for Sep. 14.

5.3 Data Preprocessing

The IR data is scaled so that all sensory observations for the learning agent are within $[0, 1]$ and all actions that learning agent can take are within $[-1, 1]$.

The IR is scaled into $[0, 1]$ corresponding to detected distance from 80cm to 10cm. The action values for all raw actuators are scaled to $[-1, 1]$. For SMAs and Moths, values in the range $[-1, 0)$ means off and values in the range $[0, 1]$ means on, while for LED the continuous values from -1 to 1 are interpreted into 0 to 255 light intensity from off to brightest. The 17 parameterized actions are scaled to $[-1, 1]$, where -1 corresponds to minimum and 1 corresponds to maximum, and their corresponding original values are shown in Table 1.

5.4 Data Analysis

The camera view includes regions outside of the LAS itself. To only focus on areas directly related to the LAS, we define three parts of the whole camera view (as shown in Fig. 8a and Fig. 8b for Camera1 and Camera2 respectively). In Fig. 8, each camera view is divided into Camera View, Whole Interest Area and Core Interest Area. For both IR Data Calibration (see Section 5.4.1) and Occupancy Estimation (see Section 5.4.2), we only consider the Whole Interest Area. Any visitors outside this interest area will be ignored for the purposes of occupancy estimation. The Core Interest Area approximates the space directly underneath the LAS.

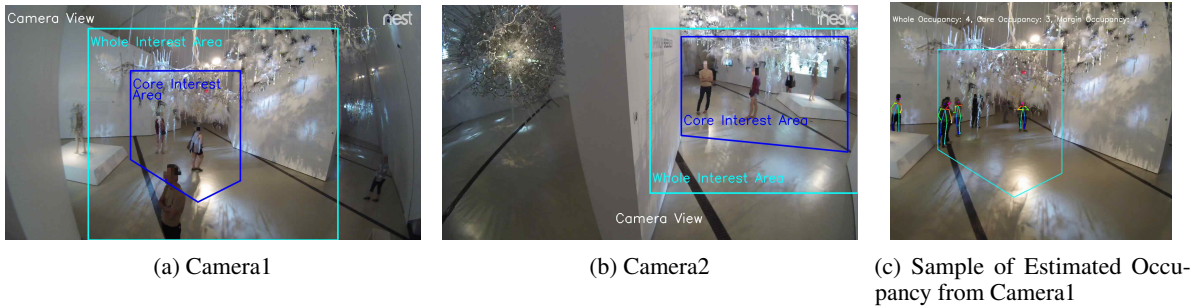


Figure 8: Interest Area Used to Estimate Occupancy

5.4.1 IR Data Calibration

To enable comparison between different behaviour modes, the sensor data must be pre-processed to ensure consistency between conditions. Since visitors can physically interact with the system, it is possible that a visitor changes the direction of the IR sensor thus changing its field of view and subsequent readings. To calibrate the IR data, two calibration steps are taken: 1) IR sensors, whose value is relatively constant and effectively not responding to occupants

(e.g., due to obstructions), are removed, 2) the baseline reading for each sensor is shifted to zero. Note that the calibration is only done for analysis, during the learning uncalibrated readings are used. To identify blocked IR and baseline shifts, we visually checked the videos recorded by the two web-cams, and selected a time period when there is no visitor within the whole interest area. Then, we find the IR data corresponding to the no-visitor time. Using the no-visitor time, we determine the thresholds for noise removal and blocked IR detection for the IR data. We use these thresholds to calibrate the raw IR data.

5.4.2 Occupancy Estimation

We also use the camera data to generate a second estimate of occupancy. We estimate the number of people occupying the space during a one minute interval, using OpenPose⁵ [57] based on the videos recorded by one of the web-cams⁶. When estimating occupancy, we only considered the Whole Interest Area.

5.4.3 Non-visitor Period Examination

We also used the camera data to determine whether there are significant periods when no visitors are present. To identify the time periods with no visitors in Whole Interest Area, we manually labelled the time periods when no person is under either camera in the Whole Interest Area. If a person's body is partially visible in Whole Interest Area, we consider it as a person being in the area. The total amount of non-visitor time throughout the experiment is 1 hour, only 2.5% of total experiment time. Therefore, we use the whole time period for analysis without removing any non-visitor intervals.

5.4.4 Estimated Engagement Level

The observation vectors used for training PLA, SARA and ACRA are different (see Section 4), so the estimated engagement, i.e., reward used for training each behaviour, cannot be directly compared. Therefore, we use raw IR readings recorded during each behaviour and Eq. 5 to calculate an estimated engagement for comparison among behaviours. Specifically, given M IR readings received within 1 minute (typically sampled at 10Hz) $\{\mathbf{ir}^{(1)}, \mathbf{ir}^{(2)}, \dots, \mathbf{ir}^{(M)}\}$ where each IR reading $\mathbf{ir}^{(i)}$ is a vector of 24 IR values, the estimated engagement level e is defined by Eq. 5:

$$e = \frac{1}{M} \frac{1}{24} \sum_{m=1}^M \sum_{i=1}^{24} \mathbf{ir}_i^{(m)} \quad (5)$$

where $\mathbf{ir}_i^{(m)}$ is the i th IR sensor in the m th IR reading. The estimated engagement is in the range $[0,1]$, where the maximum 1 corresponds to a maximally engaging state, where all IR sensors are receiving maximum readings during the entire 1 minute window, while the minimum 0 corresponds to fully non-engaging state, where all IR sensors are receiving minimum readings for the duration of the one-minute window.

5.4.5 Active Interaction Count Analysis

In addition to the estimate of engagement, we separately estimate the level of active interaction. To capture active interactions, we count the number of IR readings having value ≥ 0.25 , which corresponds to a proximity of 35cm or less from an IR sensor, within 1 minute. Formally, given M IR readings received within 1 minute (typically sampled at frequency $F = 10Hz$) $\{\mathbf{ir}^{(1)}, \mathbf{ir}^{(2)}, \dots, \mathbf{ir}^{(M)}\}$ where each IR reading $\mathbf{ir}^{(i)}$ is a vector of 24 IR values, the number of active interactions N_{active} is defined by Eq. 6:

$$N_{active} = \frac{1}{F} \sum_{m=1}^M \sum_{i=1}^{24} 1 \left\{ \mathbf{ir}_i^{(m)} \geq 0.25 \right\} \quad (6)$$

where $\mathbf{ir}_i^{(m)}$ is the i th IR sensor in the m th IR reading, and $1 \{ \cdot \}$ is an indicator function. Therefore, N_{active} is the total detected active interactions within 1 minute.

⁵<https://github.com/CMU-Perceptual-Computing-Lab/openpose>

⁶Videos from Camera2 are highly affected by the changing light of the projector as shown in Fig. 8b, so for occupancy estimation we only used videos from Camera1.

6 RESULTS

In this section, we first quantitatively compare the performance of the four behaviours based on sensory data. After that, we analyze the human survey data. Finally, we summarize the participants' qualitative feedback and researchers' observations.

6.1 Quantitative Comparison Among Four Behaviour Modes

In this section, we quantitatively compare the performance of the four behaviour modes based on sensory data collected during the interaction between visitors and the LAS. We use two ways to quantitatively compare the four behaviours' performance: 1) comparing the estimated engagement level, as described in Section 5.4.4, and 2) comparing the number of active interactions, as introduced in Section 5.4.5.

Our experiment is run in a natural setting, i.e., a publicly accessible museum, so it is possible that there are different occupancy levels in the space due to factors not related to the behaviour mode. To check whether there are different occupancy levels between conditions (which might be caused either by some behaviours being more attractive to visitors, or factors not related to system behaviours), we analyze the overall occupancy level for each behaviour mode, as described in Section 5.4.2. Fig. 9 shows a comparison of the estimated occupancy among the four behaviour modes, and Table 4 shows the results of Welch's t -test comparing the estimated occupancies between behaviours. These results illustrate that there is no significant difference between PB and PLA in terms of occupancy level, while the occupancy level difference between the other behaviour pairs is significant. Bearing this in mind, we can compare performance between PB and PLA without possibility of crowd bias, while we cannot make such unbiased comparison for other behaviour pairs. An interactive system can impact occupancy by (a) attracting new visitors, or (b) retaining existing visitors. Visitors can also be attracted to the exhibit through other means (e.g., signage in the museum, previous knowledge about the exhibit, etc.). Therefore, in the following sub-sections we will show results both on raw data and on data per average estimated occupancy, i.e., divided by average estimated occupancy, for each behaviour to provide a thorough comparison.

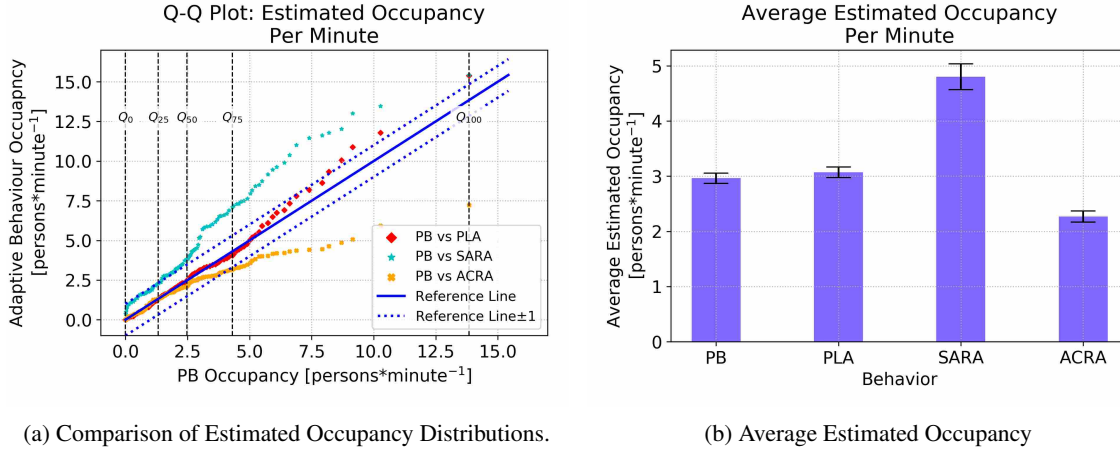


Figure 9: Estimated Occupancy Comparison. (a) is a Q-Q (100-quantiles-100-quantiles) plot of estimated per-minute occupancy, using the method introduced in Section 5.4.2, for behavior pairs (PB, PLA), (PB, SARA) and (PB, ACRA), where the coordinate (x, y) of the q -th point from bottom-left to up-right corresponds to the estimated occupancy of (PB, one of the three adaptive behaviours) for the q -th percentile, i.e. $Q_q, q = 0, 1, \dots, 100$, and the reference line indicates a perfect match of distribution between PB and one of the three adaptive behaviours. For example, the point $(4.3, 4)$ for PB vs PLA at the Q_{75} means that 75% of observations for PB and PLA are less than 4.3 and 4, respectively. (b) shows the average estimated per-minute occupancy and its standard error for each behaviour.

6.1.1 Estimated Engagement Level Comparison

Fig. 10 compares the distributions of estimated engagement (see Section 5.4.4), before and after divided by average estimated occupancy, between behaviour pairs (PB, PLA), (PB, SARA) and (PB, ACRA). From Fig. 10, we can observe that for the first 75% of data there is no noticeable difference between PB and PLA, while for the last 25% of data PLA has larger estimated engagement than PB. Since PB and PLA have similar occupancies, divided by average estimated occupancy does not influence this finding. On the other hand, SARA shows a slightly better performance than PB

Table 4: Welch's t -test on Estimated Occupancy between behaviours

	PB & PLA	PB & SARA	PB & ACRA	PLA & SARA	PLA & ACRA	SARA & ACRA
t	-0.8003	-7.0701	4.8193	-6.5955	5.4622	0.0000
p	0.4273	0.0000	0.0000	0.0000	0.0000	0.0000

Null Hypothesis: Estimated occupancy of A & B are the same. Alternate Hypothesis: Estimated occupancy of A & B are different.

(Both 1-way ANOVA and Kruskal-Wallis H-test are conducted before performing Welch's t -test. These two tests all reject their corresponding null hypothesis. Bonferroni correction is performed to counteract the problem of multiple comparisons and gives significance level $\alpha = 0.008$.)

before divided by average estimated occupancy, but shows worse performance than PB after being divided by average estimated. As for ACRA, it always shows worse performance than PB.

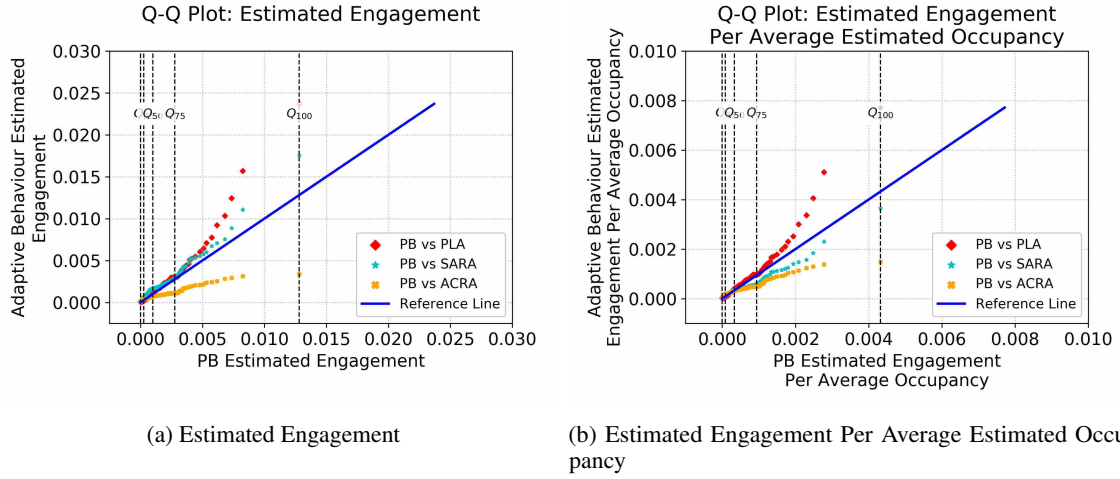


Figure 10: Estimated Engagement Distribution Comparison. (a) is a Q-Q (100-quantiles-100-quantiles) plot based on average estimated engagement, for behavior pairs (PB, PLA), (PB, SARA) and (PB, ACRA), where the coordinate (x, y) of the q -th point from bottom-left to up-right corresponds to the estimated engagement level of (PB, one of the three adaptive behaviours) for the q -th percentile, i.e. $Q_q, q = 0, 1, \dots, 100$, and the reference line indicates a perfect match of distributions between PB and one of the three adaptive behaviours. (b) is the Q-Q plot based on estimated engagement divided by average estimated occupancy.

Table 5 shows the results of the Welch's t -test on raw estimated engagement level (first two rows) and engagement level divided by average estimated occupancy (last two rows) between behaviour pairs (PB, PLA), (PB, SARA), (PB, ACRA), (PLA, SARA), (PLA, ACRA), (SARA, ACRA). Welch's t -test between PB and PLA with the null hypothesis, "*PB and PLA have identical average estimated engagement*", results in a t -statistic of -3.1743 with p -value 0.0015 for raw estimated engagement and a t -statistic of -2.6892 with p -value 0.0073 for estimated engagement divided by average estimated engagement, both rejecting the null hypothesis and indicating a statistically significant difference between PB and PLA in terms of estimated engagement. For the other behaviour pairs, PB and PLA are both consistently better than ACRA, for both raw and divided estimated engagement. However, for other behaviour pairs contrary performances are shown for raw and divided estimated engagement, e.g. PB is worse than SARA for raw estimated engagement, but shows better performance than SARA for divided estimated engagement.

Table 5: Welch's t -test on Estimated Engagement Level between Behaviours

	PB & PLA	PB & SARA	PB & ACRA	PLA & SARA	PLA & ACRA	SARA & ACRA
t	-3.1743	-2.1618	6.7400	-0.2538	9.0715	0.0000
p	0.0015	0.0321	0.0000	0.7999	0.0000	0.0000
$t_{(divided)}$	-2.6892	2.1428	3.8704	4.1507	5.9435	0.2473
$p_{(divided)}$	0.0073	0.0331	0.0002	0.0000	0.0000	0.2473

Null Hypothesis: Estimated engagement of A & B are the same. Alternate Hypothesis: Estimated engagement of A & B are different.

(Both 1-way ANOVA and Kruskal-Wallis H-test are conducted before performing Welch's t -test. These two tests all reject their corresponding null hypothesis. Bonferroni correction is performed to counteract the problem of multiple comparisons and gives significance level $\alpha = 0.008$.)

Fig. 11 shows the average estimated engagement and average estimated engagement per average occupancy. PLA achieved better performance than PB in terms of estimated engagement. SARA shows comparable average estimated engagement with PLA, but the average estimated engagement divided by average estimated occupancy is worse than PLA. ACRA is consistently worse than the other three behaviours.

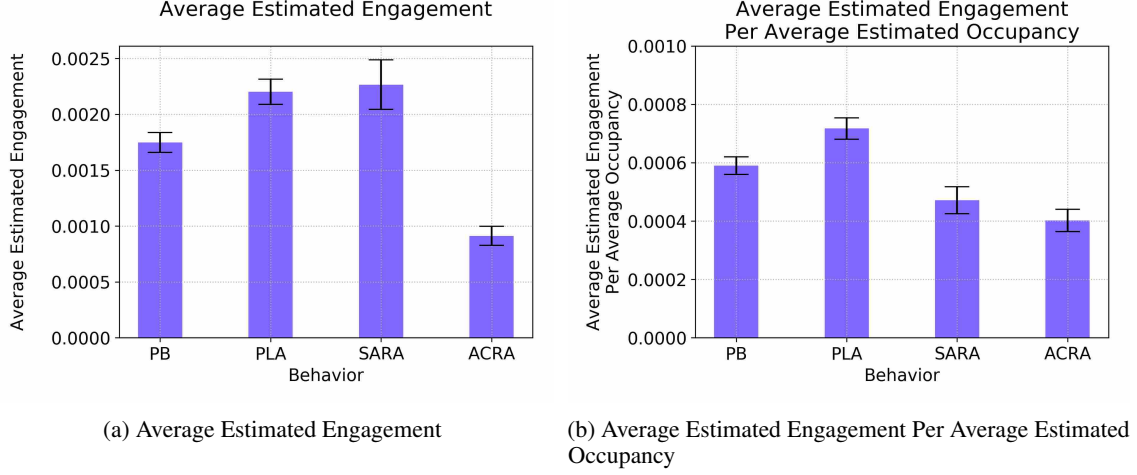


Figure 11: Average Estimated Engagement Comparison. (a) shows the average estimated engagement and its corresponding standard error. (b) shows the average estimated engagement divided by average occupancy and its corresponding standard error.

6.1.2 Active Interaction Comparison

Fig. 12 compares the distributions of active interaction count based on Eq. 6, before and after divided by average occupancy, between behaviour pairs (PB, PLA), (PB, SARA) and (PB, ACRA). From this figure, we can see that for about 50% of observations, PLA achieves higher active interaction than PB. SARA and ACRA both perform worse than PB in terms of active interaction.

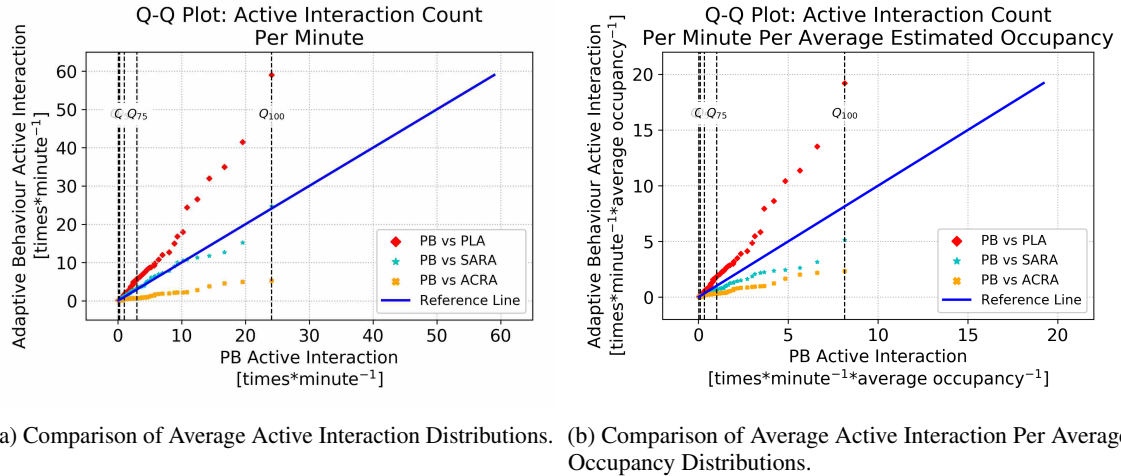


Figure 12: Active Interaction Count Comparison. (a) and (b) are Q-Q Plots based on active interaction count per minute obtained using Eq. 6. The data used in (a) is the summation of active interaction count over 1 minute, and in (b) it is then divided by average estimated occupancy. In each plot, every (x, y) corresponds to the active interaction count of (PB, one of three adaptive behaviours) in one percentile, and the reference line indicates a perfect match of distributions between PB and one of the three adaptive behaviours.

Table 6 shows the results of Welch's *t*-tests on raw active interaction counts (first two rows) and interaction counts divided by average estimated occupancy (last two rows) between behaviour pairs (PB, PLA), (PB, SARA), (PB, ACRA),

(PLA, SARA), (PLA, ACRA), (SARA, ACRA). Welch's t -test between PB and PLA with the null hypothesis, "*PB and PLA have identical average active interaction count*", results in a t -statistic of -4.5699 with p -value 0.0000 for raw estimated engagement and a t -statistic of -4.3418 with p -value 0.0000 for scaled active interaction count, both rejecting the null hypothesis and indicating a statistically significant difference between PB and PLA in terms of active interaction count. For the other behaviour pairs, PB is consistently better than ACRA and PLA is consistently better than SARA and ACRA, for both raw and scaled estimated active interaction counts. PB is better than SARA for scaled active interaction count.

Table 6: Welch's t -test on Active Interaction Count between Behaviours

	PB & PLA	PB & SARA	PB & ACRA	PLA & SARA	PLA & ACRA	SARA & ACRA
t	-4.5699	-0.2451	6.6452	3.7015	8.8043	0.0000
p	0.0000	0.8066	0.0000	0.0002	0.0000	0.0000
$t_{(divided)}$	-4.3418	2.8553	5.2314	6.2426	7.8496	0.0304
$p_{(divided)}$	0.0000	0.0046	0.0000	0.0000	0.0000	0.0304

Null Hypothesis: Active interaction count of A & B are the same. *Alternate Hypothesis:* Active interaction count of A & B are different.
(Both 1-way ANOVA and Kruskal-Wallis H-test are conducted before performing Welch's t -test. These two tests all reject their corresponding null hypothesis. Bonferroni correction is performed to counteract the problem of multiple comparisons and gives significance level $\alpha = 0.008$.)

Fig. 13 compares average active interaction counts among four behaviours ((a) average raw active interaction count and (b) average active interaction count divided by average estimated occupancy) and their corresponding standard errors. As shown in these results, PLA almost doubles the PB average active interaction count. SARA shows comparable results to PB for raw active interaction count, but a worse result for divided active interaction count. ACRA seems the worst among four behaviours in terms of active interaction.

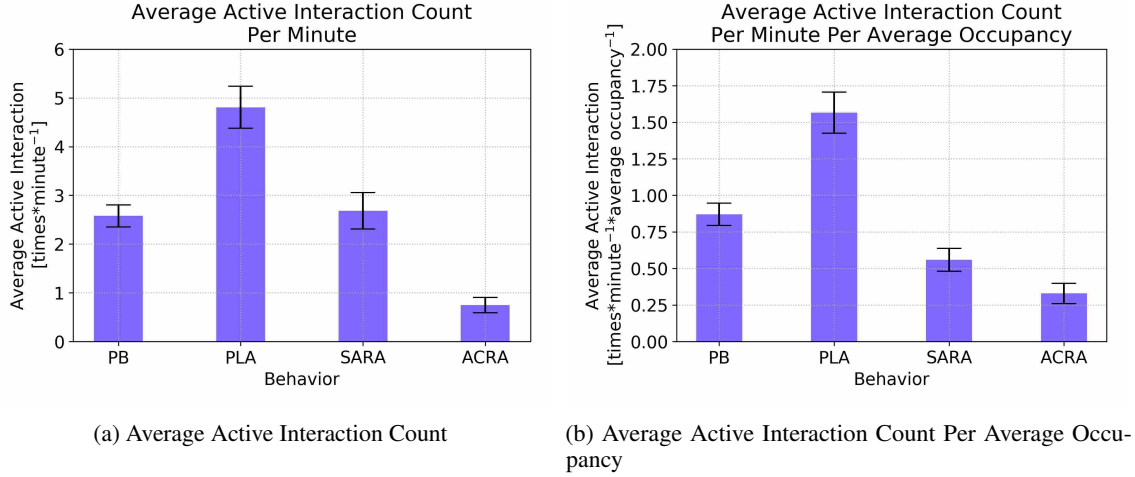


Figure 13: Average Active Interaction Count Comparison. (a) shows the average number of active interactions per minute for each behaviour, where the counting is based on 1Hz interaction frequency. (b) shows the average active interaction count per minute divided by average estimated occupancy.

6.2 Human Survey Results

In this section, we analyze the visitor responses to the survey. We focus on the survey data for PB and PLA, we omit analysis of SARA and ACRA due to the very limited number of participants (see Table 3). We first examine if there are any differences in the population characteristics between the participants who engaged with the system in PB or PLA behaviour modes. Then, we compare the PB and PLA responses for each Godspeed category. Finally, we compare PB and PLA for each Godspeed question individually, comparing the number of participants providing a rating of five.

We first analyze whether there are population differences between conditions. In Section 5.4.2, we confirmed that there were no significant differences between PB and PLA in terms of estimated occupancy. To test for differences in participant background and interest, we performed a χ^2 -test on participants' background and interests based on the first two questions in our questionnaire (see Section 5.2), and found no statistically significant differences between the two groups.

Fig. 14 shows the Box-plot and Violin-plot of the calculated average grade over each Godspeed category for PB and PLA. Within the five Godspeed categories, only *Likeability* has a relatively large gap between the medians of PB and PLA. In addition, Likeability has a relatively small variance, whereas other categories have large variance. We ran a *t*-test on the average grade and found that PLA is rated higher than PB for Likeability with 95% confidence, whereas for other categories there is no significant difference between PB and PLA.

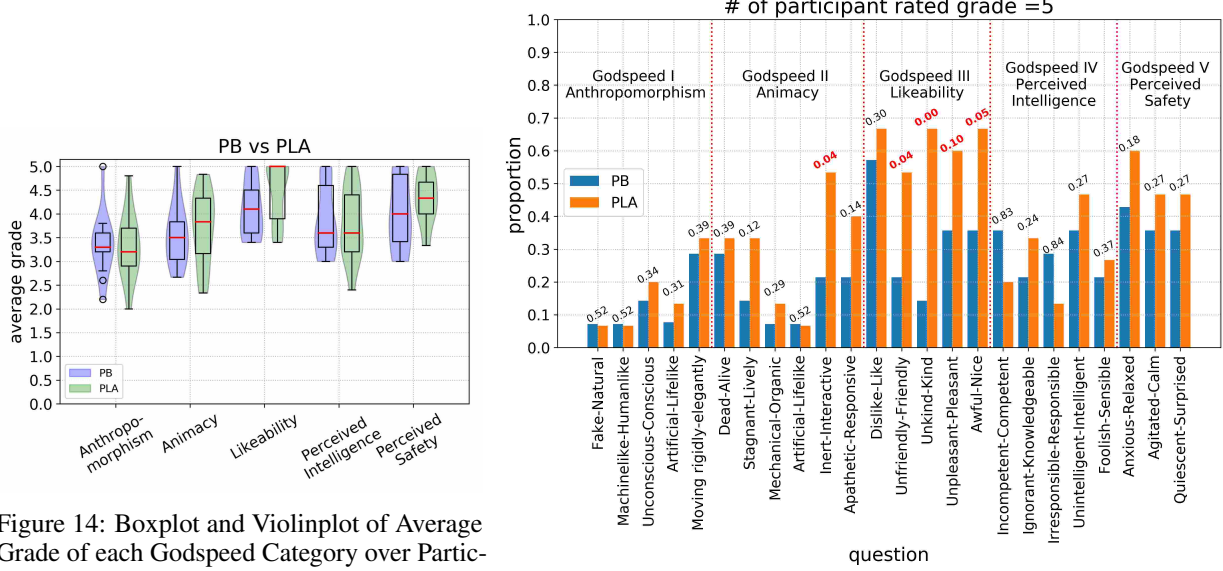


Figure 14: Boxplot and Violinplot of Average Grade of each Godspeed Category over Participants within PB or PLA.

Figure 15: Proportion of Participants who Rated with Grade=5. The value above the bars for each question is the *p* value of *z*-test with alternative hypothesis $p_{PB} < p_{PLA}$, where p_{PB} and p_{PLA} are the proportion of participants who have a = 5 rating among all participants within PB and PLA respectively.

Fig. 15 shows the proportion of participants who rated each question = 5. From this figure, we can see that there are significant differences between PB and PLA in questions related to *Godspeed III-Likeability*, whereas for most of the questions in the other four Godspeed categories, there are no statistically significant differences. Specifically, for questions *Inert-Interactive*, *Unfriendly-Friendly*, *Unkind-Kind*, *Unpleasant-Pleasant* and *Awful-Nice* PLA is better than PB with a high confidence >90%, while for the other questions there are no statistically significant differences.

In summary, PLA is rated higher than PB by the participants in terms of Likeability and interactivity, while there are no significant differences between PB and PLA in the other Godspeed categories. This conclusion further validates **H1** from the perspective of perceived likeability.

6.3 Participants' General Feedback

In this section, we discuss the participants' qualitative feedback and observations. Even though participants commonly gave generous and complimentary comments, we could still extract insights from these general comments by focusing on their key words. In Section 6.2 we ignored SARA and ACRA due to the limited sample size, but here we will include participants' general feedback as these comments could give us qualitative insights on why SARA and ACRA received less active interaction compared to PB and PLA as shown in Fig. 13.

Examples of visitor feedback for PB, PLA, SARA and ACRA are as follows:

1. PB:

- “*Very organic inspiration - felt living and biological*”
- “*Makes me feel curious, **very engaging**, want to know more. Great experience, could see application in public spaces, would love to see children's reactions*”
- “***Very interesting** and would like to understand more ...*”
- “***interesting**, but I don't understand it really.*”

2. PLA:

- *“The interplay with music was great and **added a level of immersiveness**. I enjoyed the experience. However, it was unclear to me whether the installation reacts to the people around it or whether it behaves unrelated to the people present.”*
- *“The environment create [sic] by the research project is very real, it makes people feels like those fronds are [sic] **look like real birds**, they interact with people when they move close to it. It’s a [sic] **interesting** experience and I really enjoyed it.”*
- *“So much fun. I think we stayed there the longest. Really **enjoyed interacting** with this exhibit.”*

3. SARA:

- *“The exhibit pulls you in once you connect with it and spend time getting to know it. **It isn’t an immediate feedback.**”*
- *“The exhibit **could be improved by a faster reactive** time, but the room was empty and it **would be more interactive** with more people interacting with it.”*
- *“The technical components of the display were **less responsive** to people and seemed to be on a sort of timed cycle, more variety in responses would be really cool.”*
- *“Very interesting in purpose, but I think it **could have been more interactive!** Things seemed to move **randomly**, rather than in motion with me.”*

4. ACRA:

- *“**Hope the action more smooth** or more life likely”*

As can be seen from the above responses, participants’ comments are more positive in the PB or PLA conditions, with more negative comments in the SARA and ACRA conditions. Participants in the last two behaviour modes thought that the LAS is not responsive and not interactive. This is also reflected in Fig. 12b and 13b, where SARA and ACRA received less active interactions compared with PB and PLA.

6.4 Qualitative Observations

By observing each behaviour, we found that PB and PLA generate more interactive responses because they use behaviours contingent on IR sensor triggering, while SARA and ACRA are less interactive and tend to maintain an active state such as turning on most of the LEDs and activating SMAs and Moths. Because SARA and ACRA do not appear to generate actions contingent on user behaviour, their actions are perceived to be less interactive. As a result, most visitors just stood by and looked passively after a quick active exploration. Comparing PB with PLA, PLA shows very flexible action patterns, and some are very different from PB. Specifically, one observed behaviour generated by PLA is LEDs turned on and propagated quickly from one node to another back and forth multiple times accompanying activated SMAs and Moths, which makes the LAS look like a thunderstorm. This novel behaviour illustrates that the sculpture has taken the primitives composed by the designers and evolved engaging and interesting behaviour from those. In addition, during the entire experiment, we also found some scenarios that highlight the complexity of using RL in LAS, such as interactions between visitors and the possibility that the LAS could be physically changed by touching. See Appendix A.2 for video samples and interesting scenario snapshots.

7 DISCUSSION

In this paper, we investigated how an interactive system can learn to engage with visitors in a natural setting, where no constraints are imposed on visitors and group interaction is accommodated. Relying on the standard RL framework and a novel measure of engagement as reward, three adaptive behaviours *PLA*, *SARA* and *ACRA* were compared to one pre-scripted behaviour *PB*. Our hypothesis that learned interactive behaviour could result in higher engagement, **H1**, is validated by quantitatively comparing learning and pre-scripted modes of behaviour in terms of estimated engagement, active interaction count, and human survey data. The *SARA* and *ACRA* modes were tested to examine whether learned interactive behaviour without exploiting human expertise is as effective as that of bootstrapping with parameterized action (*PLA*), which corresponds to our **H2** and is validated by comparing with *PLA* quantitatively in terms of estimated engagement, active interaction count, and human survey data, and qualitatively in terms of participants’ feedback and observation.

Creating engaging behaviours for LAS requires learning algorithms that continue to adapt rather than optimizing to a single best policy. First, the Markov Decision Process and Stationary Environment Dynamics assumptions are broken because of the complicated interaction environment. In addition, interaction time cannot be assumed to have a constant

length, and the interaction speed is bound to physical interaction and cannot be sped up. The high dimensional action space results in a difficult control problem when acting on raw actuators. In addition, since LAS is an architectural scale interactive system, perception of the environment is more complex and may need to include both proprioception and exteroception. Therefore, although we exploit a RL framework in our work, the role it plays is different from that of standard test-beds such as OpenAI Gym[58] or Arcade Learning Environment (ALE)[59]. In this work, RL is used to introduce adaptability, but there is no guarantee that the learning leads to optimal policy.

We hypothesize that the PLA configuration outperforms the other modes because it benefits from both human expert input and learning. During the design process, architects design PB based on their expertise. We exploit this human expertise to effectively restrict the parameterized action space of PLA into a region where we know good solutions can be found, and at the same time limit the dimension of the PLA action space. Therefore, PB and PLA both incorporate human intelligence. Compared with PB, PLA is endowed with adaptability by applying RL to its parameterized action space. On the other hand, SARA and ACRA do not exploit human expertise, and have very large action spaces. Even though they have maximum flexibility, they produced less satisfying results according to the user experience surveys.

The group setting presents a challenging environment for learning. In addition to those shown in Fig. 19, there are many other examples of complicated environment dynamics that present challenges to a learning algorithm. Examples include visitors who use alternate interaction strategies, change their interaction strategy over time or because they are influenced by other visitors, as well as visitors who raise their hands for reasons other than interaction. These observations illustrate the non-stationarity of the environment, and the influence of human-human interaction in group scenarios during HRI. They also emphasize the importance of developing and testing these algorithms “in the wild.”

8 CONCLUSIONS AND FUTURE WORK

In this paper, we developed and evaluated algorithms for generating interactive behaviours in group environments. Four different behaviour modes—PB, PLA, SARA and ACRA—were examined, to evaluate how the use of human knowledge and the design of the action space influence interaction. By analyzing interaction and human survey data, we found that learned interactive behaviours result in higher engagement and perceived likeability than pre-scripted behaviour. In addition, we found that learned interactive behaviours bootstrapped with parameterized action space result in higher engagement than that without exploiting human expertise. These discoveries provide a useful guideline for designing engaging behaviour for long-term interaction in similar environments.

For the future, there are several promising directions worth exploring. First, since we observed that learning in parameterized action space is easier and more engaging than on raw actuators, we could implement an agent community of PLA agents and investigate the effect of a distributed learning system, compared with centralized learning. Upcoming installations of even larger LAS are planned and this decentralization will become necessary as the number of actuated elements increases beyond one thousand in a single installation. In addition, hierarchical RL with PB bootstrapping could be a promising extension, where we could design a pool of PBs and various levels of reward functions, and see how complicated action patterns could emerge. We also plan to introduce intrinsic motivation and a learning algorithm driven both intrinsically and extrinsically for LAS. To tackle the low pace of interaction in LAS and high sample requirement of RL, we also plan to investigate how to transfer learned models from simulation to physical LAS.

ACKNOWLEDGEMENTS

The authors would like to thank Philip Beesley Architect Inc. and the Royal Ontario Museum for allowing us to conduct research with the exhibit, Salvador Breed and 4DSOUND for developing the sound system, and Joslin Goh and Pavel Shuldiner from the Statistical Consulting and Collaborative Research Unit (SCCR) at the University of Waterloo for insightful discussions on statistical analysis.

This work was supported by the Living Architecture Systems Group, funded by the Social Sciences and Humanities Research Council of Canada.

References

- [1] Candace L. Sidner, Cory D. Kidd, Christopher Lee, and Neal Lesh. Where to look: A study of human-robot engagement. In *Proceedings of the 9th International Conference on Intelligent User Interfaces*, IUI '04, pages 78–84, New York, NY, USA, 2004. ACM.

- [2] Charles Rich, Brett Ponsler, Aaron Holroyd, and Candace L Sidner. Recognizing engagement in human-robot interaction. In *2010 5th ACM/IEEE International Conference on Human-Robot Interaction (HRI)*, pages 375–382. IEEE, March 2010.
- [3] Dan Bohus and Eric Horvitz. Managing human-robot engagement with forecasts and... um... hesitations. In *Proceedings of the 16th International Conference on Multimodal Interaction, ICMI '14*, pages 2–9, New York, NY, USA, 2014. ACM.
- [4] Ginevra Castellano, André Pereira, Iolanda Leite, Ana Paiva, and Peter W. McOwan. Detecting user engagement with a robot companion using task and social interaction-based features. In *Proceedings of the 2009 International Conference on Multimodal Interfaces, ICMI-MLMI '09*, pages 119–126, New York, NY, USA, 2009. ACM.
- [5] Candace L Sidner and Christopher Lee. Engagement rules for human-robot collaborative interactions. In *SMC'03 Conference Proceedings. 2003 IEEE International Conference on Systems, Man and Cybernetics. Conference Theme - System Security and Assurance (Cat. No.03CH37483)*, volume 4, pages 3957–3962 vol.4, Oct 2003.
- [6] Rajiv Khosla, Khanh Nguyen, and Mei-Tai Chu. Human robot engagement and acceptability in residential aged care. *International Journal of Human-Computer Interaction*, 33(6):510–522, 2017.
- [7] Salvatore M Anzalone, Sofiane Boucenna, Serena Ivaldi, and Mohamed Chetouani. Evaluating the engagement with social robots. *International Journal of Social Robotics*, 7(4):465–478, Aug 2015.
- [8] Serena Ivaldi, Sébastien Lefort, Jan Peters, Mohamed Chetouani, Joelle Provasi, and Elisabetta Zibetti. Towards engagement models that consider individual factors in HRI: on the relation of extroversion and negative attitude towards robots to gaze and speech during a human-robot assembly task. *CoRR*, abs/1508.04603, 2015.
- [9] Thomas B. Sheridan. Human-robot interaction: Status and challenges. *Human Factors*, 58(4):525–532, 2016. PMID: 27098262.
- [10] Sami Haddadin and Elizabeth Croft. *Physical Human-Robot Interaction*, pages 1835–1874. Springer International Publishing, Cham, 2016.
- [11] Takayuki Kanda and Hiroshi Ishiguro. *Human-Robot Interaction in Social Robotics*. CRC Press, Inc., Boca Raton, FL, USA, 1st edition, 2012.
- [12] Panagiota Tsarouchi, Sotiris Makris, and George Chryssolouris. Human-robot interaction review and challenges on task planning and programming. *International Journal of Computer Integrated Manufacturing*, 29(8):916–931, 2016.
- [13] Michael A. Goodrich and Alan C. Schultz. Human-robot interaction: A survey. *Found. Trends Hum.-Comput. Interact.*, 1(3):203–275, January 2007.
- [14] Jakub Złotowski, Diane Proudfoot, Kumar Yogeewaran, and Christoph Bartneck. Anthropomorphism: opportunities and challenges in human-robot interaction. *International Journal of Social Robotics*, 7(3):347–360, Jan 2015.
- [15] Philip Beesley, Pernilla Ohrstedt, and Rob Gorbet. *Hylozoic Ground: Liminal Responsive Architecture: Philip Beesley*. Riverside Architectural Press, 2010.
- [16] Philip Beesley, Matthew Chan, Rob Gorbet, Dana Kulić, and Mo Memarian. Evolving systems within immersive architectural environments: New research by the living architecture systems group. *Next Generation Building*, 2:31–56, 2015.
- [17] Matthew TK Chan, Rob Gorbet, Philip Beesley, and Dana Kulić. Curiosity-based learning algorithm for distributed interactive sculptural systems. In *2015 IEEE/RSJ International Conference on Intelligent Robots and Systems (IROS)*, pages 3435–3441. IEEE, Sep. 2015.
- [18] Matthew TK Chan, Rob Gorbet, Philip Beesley, and Dana Kulić. Interacting with curious agents: User experience with interactive sculptural systems. In *2016 25th IEEE International Symposium on Robot and Human Interactive Communication (RO-MAN)*, pages 151–158. IEEE, Aug 2016.
- [19] Pierre-Yves Oudeyer and Frederic Kaplan. What is intrinsic motivation? a typology of computational approaches. *Frontiers in neurorobotics*, 1:6, 2009.
- [20] Cynthia Breazeal, Kerstin Dautenhahn, and Takayuki Kanda. *Social Robotics*, pages 1935–1972. Springer International Publishing, Cham, 2016.
- [21] Charles Isbell, Christian R. Shelton, Michael Kearns, Satinder Singh, and Peter Stone. A social reinforcement learning agent. In *Proceedings of the Fifth International Conference on Autonomous Agents, AGENTS '01*, pages 377–384, New York, NY, USA, 2001. ACM.
- [22] Andrea Lockerd Thomaz, Guy Hoffman, and Cynthia Breazeal. Real-time interactive reinforcement learning for robots. In *AAAI 2005 workshop on human comprehensible machine learning*, 2005.

- [23] Andrea L. Thomaz and Cynthia Breazeal. Reinforcement learning with human teachers: Evidence of feedback and guidance with implications for learning performance. In *Proceedings of the 21st National Conference on Artificial Intelligence - Volume 1*, AAAI'06, pages 1000–1005. AAAI Press, 2006.
- [24] Halit Bener Suay and Sonia Chernova. Effect of human guidance and state space size on interactive reinforcement learning. In *RO-MAN, 2011 IEEE*, pages 1–6. IEEE, July 2011.
- [25] W. Bradley Knox and Peter Stone. Combining manual feedback with subsequent mdp reward signals for reinforcement learning. In *AAMAS*, 2010.
- [26] W. Bradley Knox and Peter Stone. Reinforcement learning from simultaneous human and mdp reward. In *Proceedings of the 11th International Conference on Autonomous Agents and Multiagent Systems - Volume 1*, AAMAS '12, pages 475–482, Richland, SC, 2012. International Foundation for Autonomous Agents and Multiagent Systems.
- [27] Shane Griffith, Kaushik Subramanian, Jonathan Scholz, Charles L. Isbell, and Andrea Thomaz. Policy shaping: Integrating human feedback with reinforcement learning. In *Proceedings of the 26th International Conference on Neural Information Processing Systems - Volume 2*, NIPS'13, pages 2625–2633, USA, 2013. Curran Associates Inc.
- [28] Douglas G Macharet and Dinei A Florencio. Learning how to increase the chance of human-robot engagement. In *2013 IEEE/RSJ International Conference on Intelligent Robots and Systems*, pages 2173–2179, Nov 2013.
- [29] Samantha Krening and Karen M. Feigh. Interaction algorithm effect on human experience with reinforcement learning. *ACM Trans. Hum.-Robot Interact.*, 7(2):16:1–16:22, October 2018.
- [30] Kazumi Kumagai, Daiwei Lin, Lingheng Meng, Alexandru Blidaru, Philip Beesley, Dana Kulić, and Ikuo Mizuuchi. Towards individualized affective human-machine interaction. In *IEEE International Symposium on Robot and Human Interactive Communication*, pages 678–685. IEEE, IEEE, 2018.
- [31] Bilge Mutlu and Jodi Forlizzi. Robots in organizations: The role of workflow, social, and environmental factors in human-robot interaction. In *2008 3rd ACM/IEEE International Conference on Human-Robot Interaction (HRI)*, pages 287–294, March 2008.
- [32] Kotaro Hayashi, Daisuke Sakamoto, Takayuki Kanda, Masahiro Shiomi, Satoshi Koizumi, Hiroshi Ishiguro, Tsukasa Ogasawara, and Norihiro Hagita. Humanoid robots as a passive-social medium-a field experiment at a train station. In *2007 2nd ACM/IEEE International Conference on Human-Robot Interaction (HRI)*, pages 137–144. IEEE, March 2007.
- [33] Kirsikka Kaipainen, Aino Ahtinen, and Aleksi Hiltunen. Nice surprise, more present than a machine: Experiences evoked by a social robot for guidance and edutainment at a city service point. In *Proceedings of the 22Nd International Academic Mindtrek Conference*, Mindtrek '18, pages 163–171, New York, NY, USA, 2018. ACM.
- [34] Michiel Joosse and Vanessa Evers. A guide robot at the airport: First impressions. In *Proceedings of the Companion of the 2017 ACM/IEEE International Conference on Human-Robot Interaction*, HRI '17, pages 149–150, New York, NY, USA, 2017. ACM.
- [35] Chao Shi, Satoru Satake, Takayuki Kanda, and Hiroshi Ishiguro. A robot that distributes flyers to pedestrians in a shopping mall. *International Journal of Social Robotics*, 10(4):421–437, Sep 2018.
- [36] Michael Jae-Yoon Chung and Maya Cakmak. "how was your stay?": Exploring the use of robots for gathering customer feedback in the hospitality industry. In *27th IEEE International Symposium on Robot and Human Interactive Communication, RO-MAN 2018, Nanjing, China, August 27-31, 2018*, pages 947–954, 2018.
- [37] Masahiro Shiomi, Takayuki Kanda, Hiroshi Ishiguro, and Norihiro Hagita. Interactive humanoid robots for a science museum. In *Proceedings of the 1st ACM SIGCHI/SIGART Conference on Human-robot Interaction*, HRI '06, pages 305–312, New York, NY, USA, 2006. ACM.
- [38] Andrea Thomaz, Guy Hoffman, and Maya Cakmak. Computational human-robot interaction. *Found. Trends Robot*, 4(2-3):105–223, December 2016.
- [39] Kevin Doherty and Gavin Doherty. Engagement in hci: Conception, theory and measurement. *ACM Comput. Surv.*, 51(5):99:1–99:39, November 2018.
- [40] Nadine Glas and Catherine Pelachaud. Definitions of engagement in human-agent interaction. In *2015 International Conference on Affective Computing and Intelligent Interaction (ACII)*, pages 944–949, Sep. 2015.
- [41] Heather L O'Brien and Elaine G Toms. What is user engagement? a conceptual framework for defining user engagement with technology, 2008.
- [42] Marek P Michalowski, Selma Sabanovic, and Reid Simmons. A spatial model of engagement for a social robot. In *9th IEEE International Workshop on Advanced Motion Control, 2006.*, pages 762–767, March 2006.

- [43] Dan Bohus and Eric Horvitz. Models for multiparty engagement in open-world dialog. In *Proceedings of the SIGDIAL 2009 Conference*, pages 225–234. Association for Computational Linguistics, 2009.
- [44] Dan Bohus and Eric Horvitz. Open-world dialog: Challenges, directions, and a prototype. Technical report, April 2009.
- [45] Florent Levillain, Elisabetta Zibetti, and Sébastien Lefort. Interacting with non-anthropomorphic robotic artworks and interpreting their behaviour. *International Journal of Social Robotics*, 9(1):141–161, Jan 2017.
- [46] David St-Onge, Pierre-Yves Brches, Inna Sharf, Nicolas Reeves, Ioannis Rekleitis, Patrick Abouzakhm, Yogesh Girdhar, Adam Harmat, Gregory Dudek, and Philippe Gigure. Control, localization and human interaction with an autonomous lighter-than-air performer. *Robot. Auton. Syst.*, 88(C):165–186, February 2017.
- [47] David St-Onge and Nicolas Reeves. Human interaction with flying cubic automata. In *Proceedings of 2010 IEEE/ACM Internations Conference on Human Robots Interaction*, 2010.
- [48] Catie Cuan, Ishaan Pakrasi, and Amy LaViers. Time to compile. In *Proceedings of the 5th International Conference on Movement and Computing, MOCO ’18*, pages 53:1–53:4, New York, NY, USA, 2018. ACM.
- [49] Graham Wakefield, Tobias Hollerer, JoAnn Kuchera-Morin, Charles Roberts, and Matthew Wright. Spatial interaction in a multiuser immersive instrument. *IEEE computer graphics and applications*, 33(6):14–20, Nov 2013.
- [50] Federico Augugliaro, Angela P. Schoellig, and Raffaello D’Andrea. Dance of the flying machines: Methods for designing and executing an aerial dance choreography. *IEEE Robotics Automation Magazine*, 20(4):96–104, Dec 2013.
- [51] Ryan Lowe, Yi Wu, Aviv Tamar, Jean Harb, Pieter Abbeel, and Igor Mordatch. Multi-agent actor-critic for mixed cooperative-competitive environments. *CoRR*, abs/1706.02275, 2017.
- [52] Timothy P. Lillicrap, Jonathan J. Hunt, Alexander Pritzel, Nicolas Heess, Tom Erez, Yuval Tassa, David Silver, and Daan Wierstra. Continuous control with deep reinforcement learning. *CoRR*, abs/1509.02971, 2015.
- [53] David Silver, Guy Lever, Nicolas Heess, Thomas Degris, Daan Wierstra, and Martin Riedmiller. Deterministic policy gradient algorithms. In Eric P. Xing and Tony Jebara, editors, *Proceedings of the 31st International Conference on Machine Learning*, volume 32 of *Proceedings of Machine Learning Research*, pages 387–395, Beijing, China, 22–24 Jun 2014. PMLR.
- [54] Yan Duan, Xi Chen, Rein Houthoofd, John Schulman, and Pieter Abbeel. Benchmarking deep reinforcement learning for continuous control. *CoRR*, abs/1604.06778, 2016.
- [55] Arthur Juliani, Vincent-Pierre Berges, Esh Vckay, Yuan Gao, Hunter Henry, Marwan Mattar, and Danny Lange. Unity: A general platform for intelligent agents. *CoRR*, abs/1809.02627, 2018.
- [56] Christoph Bartneck, Dana Kulić, Elizabeth Croft, and Susana Zoghbi. Measurement instruments for the anthropomorphism, animacy, likeability, perceived intelligence, and perceived safety of robots. *International journal of social robotics*, 1(1):71–81, Jan 2009.
- [57] Zhe Cao, Tomas Simon, Shih-En Wei, and Yaser Sheikh. Realtime multi-person 2d pose estimation using part affinity fields. *CoRR*, abs/1611.08050, 2016.
- [58] Greg Brockman, Vicki Cheung, Ludwig Pettersson, Jonas Schneider, John Schulman, Jie Tang, and Wojciech Zaremba. Openai gym. *CoRR*, abs/1606.01540, 2016.
- [59] Marc G. Bellemare, Yavar Naddaf, Joel Veness, and Michael Bowling. The arcade learning environment: An evaluation platform for general agents. *CoRR*, abs/1207.4708, 2012.
- [60] Prafulla Dhariwal, Christopher Hesse, Oleg Klimov, Alex Nichol, Matthias Plappert, Alec Radford, John Schulman, Szymon Sidor, Yuhuai Wu, and Peter Zhokhov. Openai baselines. <https://github.com/openai/baselines>, 2017.
- [61] Matthias Plappert, Rein Houthoofd, Prafulla Dhariwal, Szymon Sidor, Richard Y. Chen, Xi Chen, Tamim Asfour, Pieter Abbeel, and Marcin Andrychowicz. Parameter space noise for exploration. *CoRR*, abs/1706.01905, 2017.

A Supplementary Materials

A.1 Implementation Details for Each Adaptive Behaviour

A.1.1 PLA

PLA uses the DDPG agent from OpenAI’s Baselines package[60]. The structure of the neural network is shown in Fig. 16. All layers are dense layers, with layer-norm applied and ReLu as the activation function. The number under each

layer indicates the neurons in that layer. tanh is used at the output layer. PLA uses parameter noise as its exploration strategy. At the start of each episode, parameter noise adds adaptive noise to the parameters of the neural network policy, rather than to its action space. This noise is fixed through out the episode[61].

Note that the exploration strategy used for PLA is different from the one used for SARA and ACRA, namely ϵ -greedy. Compared with PLA whose action dimension is 11, SARA and agents in ACRA have a larger action space, i.e., 192 and 64 respectively, we used ϵ -greedy to speed up global exploration. It is reasonable, because PLA has already narrowed down its exploration space.

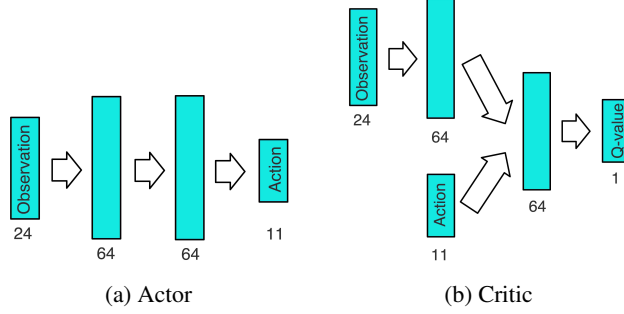


Figure 16: Actor-Critic of PLA

A.1.2 SARA

The neural network structure for SARA’s actor-critic agent is shown in Fig. 17, where the number under each layer is the neural units in that layer. The neural network is fully-connected with layer-norm applied. All hidden layers use ReLu activation function and output layer uses tanh activation function. The exploration strategy for SARA is ϵ -greedy in which the *epsilon* parameter is reset to 0.5 and discounted to 0.05 with discount rate 0.9 everyday. The reason we choose a different exploration for SARA from PLA is to speed up the exploration, because of the much larger action dimensions for SARA compared with PLA. We assume the environment dynamics is non-stationary, so our LAS must keep exploring. Therefore, on each day ϵ will be reset and discounted to 0.05, but the learned actor-critic model is continuously trained, i.e., not learning from scratch.

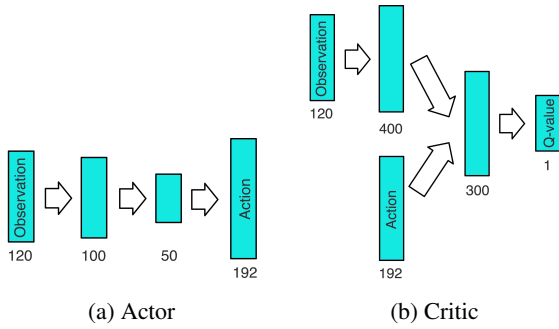


Figure 17: Actor-Critic of SARA

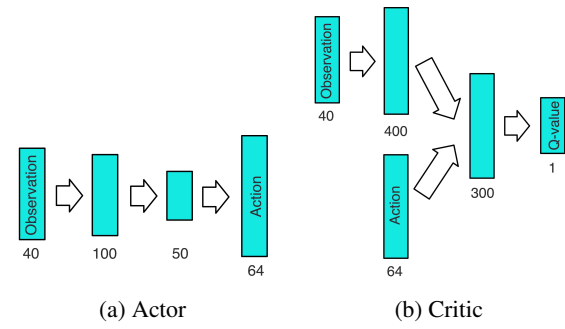


Figure 18: Actor-Critic of ACRA

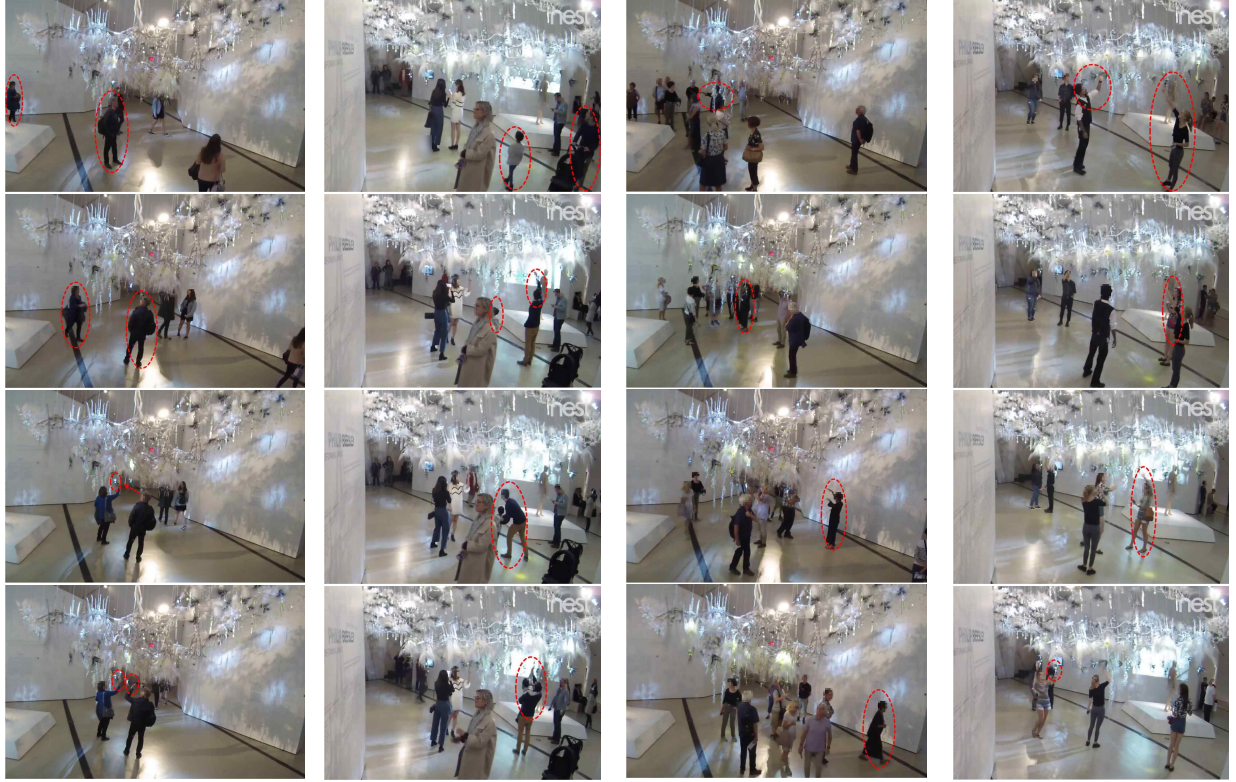
A.1.3 ACRA

ACRA has three agents, but each agent shares the same structure of neural network for actor-critic as shown in Fig. 18 and the same exploration strategy. Except for the difference in the size of observation and action space, agents in ACRA have the same structure, activation functions and exploration strategy as the agent in SARA.

A.2 Video Samples and Interesting Scenario Snapshots

Videos to compare four behaviours general behaviour features can be found in <https://youtu.be/2tICanYEpo0>, Fig. 19 shows some samples of interesting scenario:

- Fig. 19a shows how visitors can affect each other. Before the woman in blue arrives, the man in black had spent a while just looking around and did not know how to interact with the LAS. Then coincidentally he saw how the woman raised her hand and how the LAS responded. After that he copied her action to interact with the LAS.
- Fig. 19b shows a parent helping his child experience the interaction after he explored how to interact. Since the child could not reach the IR sensor, the parent lifted his child.
- Fig. 19c shows a group visit where a group of visitors is led by a guide.
- Fig. 19d shows a more complex scenario about misunderstanding shared information. In this case, three girls were taking photos without interacting. Then a security guard taught one of the three girls how to interact. At the same time, the second girl saw and joined them. After that the third girl learned this from her friends. However, there was a misunderstanding of the security guard's instruction, so they directly touched the IR sensors rather than just waving hand closely.



(a) Learn how to interact from other visitor

(b) Parent lifts child

(c) Group visit lead by a guide

(d) Visitors taught by security guard but misunderstood touch IR sensors

Figure 19: Sample Interesting Scenario